Event-Triggered Neuro-Adaptive Control for a Disturbed Non-holonomic Multi-Agents System

V. García-Cervantes[1], J. Escareno[1], D. Soto-Guerrero[1] and O. Labbani-Igbida[1]

***Abstract*— The present work lies within sustainable agricultural framework. This manuscript proposes a control strategy for a fleet of robots to grapple energy and navigation issues. In this regard, this work presents a robust neuro-adaptive controller to fulfill the tracking objective for a non-holonomic mobile multi-agent system (MAS) subject to uncertainties within a leader-follower policy. Furthermore, targeting optimal processing/communication the controller is driven by an events mechanism. Likewise, we extend non-holonomic dynamic model that include couplings, parametric uncertainties and exogenous disturbances as well. As caused by challenging terrain conditions or adverse atmospheric influences, those disturbances are approximated by using RBF NNs. Due to the limited computing resources in real applications, the event-triggered controller is synthesised considering the leader-follower scheme guaranteeing Lyapunov's closed-loop stability and avoiding Zeno phenomenon. The numerical results shows the effectiveness of the proposed control scheme.**

I. INTRODUCTION

We are currently facing different environmental challenges, mainly due to the use of techniques based on mass production, without taking into account the impact they have on the environment. The excessive use of pesticides and artificial fertilizers has led to a significant number of environmental problems. For this reason, novel alternatives are now being sought from a sustainable approach. Agricultural robotics has the potential to support agroecological objectives. The integration of agricultural robot fleets, intelligent sensors, autonomous vehicles, and computational sensing systems can enable agriculture that aligns with agroecological principles. This approach can reduce the use of chemical inputs and optimize labor times without compromising sustainability. These technologies facilitate tasks such as planting, weeding, harvesting, and crop monitoring with precision and efficiency, thereby complementing agroecological practices.

Multi-agent systems (MAS) research represents one of the most appealing topics within the fields of robotics and control theory. In this regard, it is well known that collective intelligence offers inherent benefits, including scalability, fault tolerance, and adaptability in uncertain dynamic environments [1], [2]. Synchronization and coordination are critical aspects of MAS applications, this permits collective time-parameterized agreements. Despite the numerous advantages offered by this type of systems, it comes with a significant amount of scientific challenges. Particularly for ground vehicles, control from a non-holonomic perspective becomes challenging due to its non-linearity and constraints, even more so when external disturbances are considered. Current approaches seek to achieve an optimal balance between efficiency and robustness. Consequently, the majority of these approaches involve the integration of various techniques, including robust/adaptive control, distributed observers, and event-based control. Disturbances such as sensor noise, parametric uncertainties, external forces, and actuator failures can significantly degrade the performance of the MAS or even cause instability [2], [3], [4], [5].

There are numerous studies using different adaptive control techniques in MAS, radial basis function neural networks (RBF NNs) are commonly employed to approximate the unknown disturbances in systems. Their capacity to adapt contributes significantly to the compensation of exogenous disturbances. In contrast to classical approaches featuring fixed gains, neuro-adaptive controls approximate disturbances and unknown uncertainties [3], [6], [7], [8], [9], [10]. In terms of energy efficiency, event-based approaches reduce computational and communication overhead by updating control signals only when necessary. The event trigger mechanism determines when new information should be transmitted based on predefined error conditions, reducing messages between agents while maintaining performance in the face of disturbances [11], [12], [13], [14], [15].

In this paper, we propose a neuro-adaptive controller driven by asynchronous events. This controller is designed to fulfill the tracking problem of a multi-agent system composed of a finite collection of non-holonomic ground robots for agricultural tasks. A set of time-parametrized waypoints were used to determine the MAS commanded trajectory. The exogenous disturbances arise from uneven terrain or weather conditions, we represent that as external forces that interact with the robot as it moves along the desired trajectory. The main contributions of this paper are listed below:

- Based on the general kinematics of non-holonomic systems, we derive the full multi-agent dynamics that is used to apply Backstepping technique to sithesize a robust controller for the MAS.
- External disturbances exerted upon the multi-robot system are estimated via a neuro-adaptive approach leveraging RBF-NNs. Moreover, the overall stability analysis of the event-triggered controller is demonstrated by means of Lyapunov theory, along the lack of Zeno's behavior.

This work has benefited from French state aid managed by the National Research Agency under the France 2030 program, with reference ANR-22-PEAE-0007.

[1] Robotics and Mechatronics Department, XLIM Research Institute UMR-CNRS 87060, University of Limoges, France.

The remainder of the paper is organized as follows: section II provides the theoretical basis related to MAS. The mathematical model is outlined is section III presents the mathematical model. The neuro-adaptive control scheme is detailed by section IV. This is followed by the section presenting the numerical results assessing the effectiveness of the control strategy within a disturbed scenario in V. Finally, the concluding remarks and forthcoming research are presented in section VI.

II. Theoretical Prerequisites

A. Graph Theory

The MAS can be conceptualized as a collection of dynamic entities (or agents) that present a specific communication policy, fixed or time-varying, called topology. As demonstrated in [16], [17] a directed graph can be represented as $\mathcal{G} = \{\mathcal{V}, \mathcal{E}, \mathcal{A}\}$. $\mathcal{G}$ is structured from a nonempty set containing a finite number of vertices or nodes $\mathcal{V} = 1, 2, ..., N$. $\mathcal{E}$ is an edge set defined as follows $\mathcal{E} = (i, j) \forall i, j \in \mathcal{V}$, where (i, j) indicate that the node j can obtain information from the node i. The adjacency matrix is defined as $\mathcal{A} = a(i, j) \in \mathbb{R}^{N \times N}$ where the element $a(i, j) \in \mathbb{R}^+ \iff (i, j) \in \mathcal{E}$ and $a(i, j) = 0$ otherwise. The in-degree and out-degree of node i are respectively represented as $\deg_{in}(i) = \sum_{j=1}^{N} a_{ij}$ and $\deg_{out}(i) = \sum_{j=1}^{N} a_{ji}$. The set of neighbors of agent i is denoted by $\mathcal{N}_i = \{j : (i, j) \in \mathcal{V}\}$ The Laplacian matrix $\mathcal{L}$ is represented as $\mathcal{L} = \mathcal{D} - \mathcal{A}$, where the diagonal matrix $\mathcal{D} = \mathrm{diag}(d_1, d_2, ...d_n)$ is conformed by elements $\sum_{j=1}^{n} a(i, j)$, see [18], [19]. If every node in the graph contains a directed path to all other distinct nodes in $\mathcal{V}$, then the direct graph is said to have a spanning tree. Furthermore, for describing the interaction between a leader agent 0 and N followers, we use $\mathcal{B}$ which is a diagonal matrix with entries 1, just if there is an edge between the leader and any other agent in the group, and 0 otherwise. Matrix $\mathcal{H} = \mathcal{L} + \mathcal{B}$ has full rank when $\mathcal{G}$ has a spanning tree with leader as the root, which implies non singularity of $\mathcal{H}$.

B. Function Approximation with Neural Networks

Theorem 1. *(Universal approximation) Let $f(x(t))$ be a smooth function with $x(t)$ in the compact set Ω. Thus, there exists a neural network (NN) of η neurons satisfying*

$$f(x(t)) = \boldsymbol{\omega}^T \boldsymbol{\varphi}(x(t)) + \varepsilon \;\forall x(t) \in \Omega \tag{1}$$

where $\boldsymbol{\omega} \in \mathbb{R}^\eta$ the NN weight vector, $\boldsymbol{\varphi}(x(t)) \in \mathbb{R}^\eta$ represents the activation function and ε the approximation error. In this study, we consider radial basis functions (RBF) as the activation function, therefore $\varphi_i = exp\left(-\|x(t) - \boldsymbol{\mu}_i\|^2/\sigma^2\right)$, where $x(t)$ is the input of the NN, $\boldsymbol{\mu}_i = (\mu_1, \mu_2, \ldots, \mu_\eta)^T \in \mathbb{R}^\eta$ defines the mean value of the basis node, while σ refers to the width of the base node. Let the optimal weight $\boldsymbol{\omega}^\star$

$$\boldsymbol{\omega}^\star := \underset{\boldsymbol{\omega} \in \Omega \subset \mathbb{R}^\eta}{\arg\min} \left\{\|f(x(t)) - \boldsymbol{\omega}^T \boldsymbol{\varphi}(x(t))\|^2\right\} \tag{2}$$

Therefore, the optimal approximation of $f(x(t))$ is expressed as $f^\star(x(t)) = {\boldsymbol{\omega}^\star}^T \boldsymbol{\varphi}(x(t)) + \varepsilon$ where $\boldsymbol{\omega}^\star = [\omega_1^\star, \ldots, \omega_\eta^\star]^T$ and $\boldsymbol{\varphi} = [\varphi_1, \ldots, \varphi_\eta]^T$. And are upper-bounded as $\|\boldsymbol{\omega}^\star\| \leq \bar{\omega}$, $\|\boldsymbol{\varphi}(\cdot)\| \leq \bar{\varphi}$ and $|\varepsilon| \leq \bar{\varepsilon}$, with $\bar{\omega}$, $\bar{\varphi}$, and $\bar{\varepsilon}$ constants $\in \mathbb{R}^+$. The optimal approximation can be represented as $\hat{f}(x(t)) = \hat{\boldsymbol{\omega}}^T \boldsymbol{\varphi}(x(t))$ with $\hat{\boldsymbol{\omega}} = [\hat{\omega}_1, \ldots, \hat{\omega}_\eta]^T$.

III. Dynamic Modeling

A. Tracking of a simplified dynamic model

The vehicle's motion is directly dependent on its posture $\boldsymbol{p}(t) = \begin{bmatrix} x(t) & y(t) & \phi(t) \end{bmatrix}^T$. Here $x(t)$ and $y(t)$ represent the location of the midpoint between the rear wheels, while $\phi(t)$ represents the heading direction. The vehicle's controls are the translational velocity $v(t)$ and the rotational velocity $w(t)$ as shown in Fig. 1. The simplified kinematics of one vehicle is $\dot{\boldsymbol{p}} = \begin{bmatrix} v\cos\phi & v\sin\phi & w \end{bmatrix}^T$. The problem we are addressing is the tracking problem, defined as the search for control laws v and w such that the robot follows a reference trajectory given by the posture $p_d(t) = \begin{bmatrix} x_d(t) & y_d(t) & \phi_d(t) \end{bmatrix}^T$ and inputs $\begin{bmatrix} v_d(t) & w_d(t) \end{bmatrix}^T$.

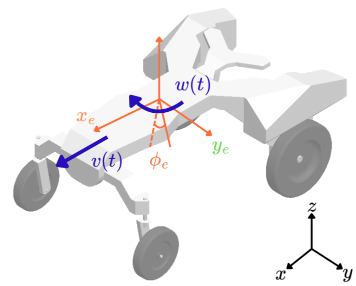

Fig. 1: Ackermann model.

The proposed MAS control strategy aims to achieve consensus while rejecting external disturbances. The virtual leader is responsible for providing the desired posture to each follower, which comes from the desired trajectory. The MAS must achieve leader-following consensus, i.e.,

$$\lim_{t \to \infty} ||\boldsymbol{p}_i - \mathbf{1}_n \otimes \boldsymbol{p}_d - \boldsymbol{p}_f|| \to 0, \tag{3}$$

where $\boldsymbol{p}_i \in \mathbb{R}^{mn}$, $\boldsymbol{p}_d \in \mathbb{R}^m$ and $\boldsymbol{p}_f \in \mathbb{R}^{mn}$ (in our case $m = 3$) are the position vectors of the $i - th$ follower, the virtual leader and the desired formation respectively. The kinematics for the $i - th$ agent can be rewritten as:

$$\dot{\boldsymbol{p}}_{\boldsymbol{i}} = \begin{bmatrix} \dot{x}_i \\ \dot{y}_i \\ \dot{\phi}_i \end{bmatrix} = \begin{bmatrix} \mathrm{C}_{\phi_i} & \mathbf{0}_n \\ \mathrm{S}_{\phi_i} & \mathbf{0}_n \\ \mathbf{0}_n & \mathbf{1}_n \end{bmatrix} \begin{bmatrix} v_i \\ w_i \end{bmatrix}, \tag{4}$$

where $\mathrm{C}_\star = \cos(\star)$ and $\mathrm{S}_\star = \sin(\star)$. Let us now consider the accumulated tracking errors for the vehicle, which in terms of graph theory these are given as follows,

$$\boldsymbol{e}_{pi}(t) = \begin{bmatrix} e_{xi}(t) \\ e_{yi}(t) \\ e_{\phi i}(t) \end{bmatrix} = \begin{bmatrix} \mathcal{H}(x_{di} - \bar{x}_i) \\ \mathcal{H}(y_{di} - \bar{y}_i) \\ \mathcal{H}(\phi_{di} - \bar{\phi}_i) \end{bmatrix} \in \mathbb{R}^{3n}, \tag{5}$$

where:

- $e_{xi}(t) = \begin{bmatrix} e_{x1}(t), & \ldots, & e_{xn}(t) \end{bmatrix}^T$
- $\bar{x}_i = \begin{bmatrix} x_1(t) - x_{f1}, & \ldots, & x_n(t) - x_{fn} \end{bmatrix}^T$
- $x_{di} = \begin{bmatrix} \mathbf{1}_n \otimes x_{d1}(t), & \ldots, & \mathbf{1}_n \otimes x_{dn}(t) \end{bmatrix}^T$

and their respective equivalents for the state variables y and ϕ (the desired formation for the angle ϕ must be $\phi_{fi} = \mathbf{0}_n$).

Lemma 1. *The error dynamics for the $i-th$ agent is:*

$$\begin{bmatrix} \dot{x}_{ei} \\ \dot{y}_{ei} \\ \dot{\phi}_{ei} \\ \dot{v}_i \\ \dot{w}_i \end{bmatrix} = \begin{bmatrix} w_i \odot y_{ei} + \mathcal{H}(-v_i + v_{di} \odot C_{\phi_{ei}}) \\ -w_i \odot x_{ei} + \mathcal{H}(v_{di} \odot S_{\phi_{ei}}) \\ \mathcal{H}(w_d - w_i) \\ u_{vi}(t) + \delta_{vi}(t) \\ u_{wi}(t) + \delta_{wi}(t) \end{bmatrix}. \tag{6}$$

Proof. Based on the work of [20] and [21], the following structure is obtained for the MAS. Considering the global consensus error (5), we can obtain the body frame posture error for the $i-th$ agent as $\boldsymbol{p}_{ei}(t) = \mathrm{R}_{\phi_i} \boldsymbol{e}_{pi}(t)$,

$$\begin{bmatrix} x_{ei} \\ y_{ei} \\ \phi_{ei} \end{bmatrix} = \begin{bmatrix} \mathrm{C}_{\phi_i} & \mathrm{S}_{\phi_i} & \mathbf{0}_n \\ -\mathrm{S}_{\phi_i} & \mathrm{C}_{\phi_i} & \mathbf{0}_n \\ \mathbf{0}_n & \mathbf{0}_n & \mathbf{1}_n \end{bmatrix} \begin{bmatrix} \mathcal{H}(x_{di} - \bar{x}_i) \\ \mathcal{H}(y_{di} - \bar{y}_i) \\ \mathcal{H}(\phi_{di} - \bar{\phi}_i) \end{bmatrix}. \tag{7}$$

The time derivative $\dot{\boldsymbol{p}}_{ei}(t) = \dot{\mathrm{R}}_{\phi_i} \boldsymbol{e}_{pi}(t) + \mathrm{R}_{\phi_i} \dot{\boldsymbol{e}}_{pi}(t)$ is obtained using (7) and the non-holonomic restrictions $\dot{x}_{di}\mathrm{S}_{\phi_{di}} = \dot{y}_{di}\mathrm{C}_{\phi_{di}}$ from (4).

$$\begin{aligned} \dot{x}_{ei} =& -\mathcal{H}(x_{di} - \bar{x}_i)\dot{\phi}_i \odot \mathrm{S}_{\phi_i} + \mathcal{H}(y_{di} - \bar{y}_i)\dot{\phi}_i \odot \mathrm{C}_{\phi_i} \\ &+ \mathcal{H}(\dot{x}_{di} - \dot{\bar{x}}_i) \odot \mathrm{C}_{\phi_i} + \mathcal{H}(\dot{y}_{di} - \dot{\bar{y}}_i) \odot \mathrm{S}_{\phi_i} \\ =& w_i \odot y_{ei} - \mathcal{H}(\dot{\bar{x}}_i \odot \mathrm{C}_{\phi_i} + \dot{\bar{y}}_i \odot \mathrm{S}_{\phi_i}) \\ &+ \mathcal{H}(\dot{x}_{di} \odot \mathrm{C}_{\phi_i} + \dot{y}_{di} \odot \mathrm{S}_{\phi_i}) \\ =& w_i \odot y_{ei} - \mathcal{H}v_i + \mathcal{H}(\dot{x}_{di} \odot \mathrm{C}_{\phi_{di}-\phi_{ei}} + \dot{y}_{di} \odot \mathrm{S}_{\phi_{di}-\phi_{ei}}) \\ =& w_i \odot y_{ei} - \mathcal{H}v_i + \mathcal{H}[\dot{x}_{di} \odot (\mathrm{C}_{\phi_{di}} \odot \mathrm{C}_{\phi_{ei}} + \mathrm{S}_{\phi_{di}} \odot \mathrm{S}_{\phi_{ei}}) \\ &+ \dot{y}_{di} \odot (\mathrm{S}_{\phi_{di}} \odot \mathrm{C}_{\phi_{ei}} - \mathrm{C}_{\phi_{di}} \odot \mathrm{S}_{\phi_{ei}})] \\ =& w_i \odot y_{ei} - \mathcal{H}v_i + \mathcal{H}[(\dot{x}_{di} \odot \mathrm{C}_{\phi_{di}} + \dot{y}_{di} \odot \mathrm{S}_{\phi_{di}}) \odot \mathrm{C}_{\phi_{ei}} \\ &+ (\dot{x}_{di} \odot \mathrm{S}_{\phi_{di}} - \dot{y}_{di} \odot \mathrm{C}_{\phi_{di}}) \odot \mathrm{S}_{\phi_{ei}}] \\ =& w_i \odot y_{ei} - \mathcal{H}v_i + \mathcal{H}(v_{di} \odot \mathrm{C}_{\phi_{ei}}) \\ =& w_i \odot y_{ei} + \mathcal{H}(-v_i + v_{di} \odot \mathrm{C}_{\phi_{ei}}), \end{aligned}$$

$$\begin{aligned} \dot{y}_{ei} =& -\mathcal{H}(x_{di} - \bar{x}_i)\dot{\phi}_i \odot \mathrm{C}_{\phi_i} - \mathcal{H}(y_{di} - \bar{y}_i)\dot{\phi}_i \odot \mathrm{S}_{\phi_i} \\ &- \mathcal{H}(\dot{x}_{di} - \dot{\bar{x}}_i) \odot \mathrm{S}_{\phi_i} + \mathcal{H}(\dot{y}_{di} - \dot{\bar{y}}_i) \odot \mathrm{C}_{\phi_i} \\ =& -w_i \odot x_{ei} + \mathcal{H}(\dot{\bar{x}}_i \odot \mathrm{S}_{\phi_i} - \dot{\bar{y}}_i \odot \mathrm{C}_{\phi_i}) \\ &+ \mathcal{H}(-\dot{x}_{di} \odot \mathrm{S}_{\phi_i} + \dot{y}_{di} \odot \mathrm{C}_{\phi_i}) \\ =& -w_i \odot x_{ei} + \mathcal{H}(-\dot{x}_{di} \odot \mathrm{S}_{\phi_{di}-\phi_{ei}} + \dot{y}_{di} \odot \mathrm{C}_{\phi_{di}-\phi_{ei}}) \\ =& -w_i \odot x_{ei} + \mathcal{H}[-\dot{x}_{di} \odot (\mathrm{S}_{\phi_{di}} \odot \mathrm{C}_{\phi_{ei}} - \mathrm{C}_{\phi_{di}} \odot \mathrm{S}_{\phi_{ei}}) \\ &+ \dot{y}_{di} \odot (\mathrm{C}_{\phi_{di}} \odot \mathrm{C}_{\phi_{ei}} + \mathrm{S}_{\phi_{di}} \odot \mathrm{S}_{\phi_{ei}})] \\ =& -w_i \odot x_{ei} + \mathcal{H}[(-\dot{x}_{di} \odot \mathrm{S}_{\phi_{di}} + \dot{y}_{di} \odot \mathrm{C}_{\phi_{di}}) \odot \mathrm{C}_{\phi_{ei}} \\ &+ (\dot{x}_{di} \odot \mathrm{C}_{\phi_{di}} + \dot{y}_{di} \odot \mathrm{S}_{\phi_{di}}) \odot \mathrm{S}_{\phi_{ei}}] \\ =& -w_i \odot x_{ei} + \mathcal{H}(v_{di} \odot \mathrm{S}_{\phi_{ei}}), \end{aligned}$$

Finally, it is evident that $\dot{\phi}_{ei} = \mathcal{H}(\dot{\phi}_{di} - \dot{\bar{\phi}}_i) = \mathcal{H}(w_{di} - w_i)$. The symbol $\odot$ denotes the piece-wise element product, $v_{di} = \mathbf{1}_n \otimes v_d$, and $w_{di} = \mathbf{1}_n \otimes w_d$. We define $\dot{v}_i = u_{vi}(t) + \delta_{vi}(t)$ and $\dot{w}_i = u_{wi}(t) + \delta_{wi}(t)$, where $u_{vi}(t) \in \mathbb{R}^n$ and $u_{wi}(t) \in \mathbb{R}^n$ are the torques or generalized force variables of the MAS and the external disturbances in the vehicles are represented by $\delta_{vi}(t) \in \mathbb{R}^n$ and $\delta_{wi}(t) \in \mathbb{R}^n$$\square$.

IV. Control Design

A. MAS Backstepping Tracking Control

Backstepping technique initially stabilizes the first integrator dynamics (6a), (6b) and (6c) through the virtual inputs v_i^v and w_i^v :

$$v_i^v = \mathcal{H}^{-1} K_x x_{ei} + v_{di} \odot \mathrm{C}_{\phi_{ei}} \tag{8}$$
$$w_i^v = \mathcal{H}^{-1} K_\phi \phi_{ei} + w_{di} + v_{di} \odot y_{ei}, \tag{9}$$

with $K_x, K_\phi > 0$. Since these inputs are not available, thus for the next step these virtual inputs are used as references $\alpha_{vi} \triangleq v_i^v$ and $\alpha_{wi} \triangleq w_i^v$ to encode the error variables $z_{vi}(t) = v_i - \alpha_{vi}(t)$ and $z_{wi}(t) = w_i - \alpha_{wi}(t)$ for the translational and rotational motion, respectively. The time differentiation of the auxiliary variables results in the following equations: $\dot{z}_{vi}(t) = \dot{v}_i - \dot{\alpha}_{vi}(t)$ and $\dot{z}_{wi}(t) = \dot{w}_i - \dot{\alpha}_{wi}(t)$, where,

$$\begin{aligned} \dot{\alpha}_{vi}(t) &= \mathcal{H}^{-1} K_x \dot{x}_{ei} + \dot{v}_{di} \odot \mathrm{C}_{\phi_{ei}} - v_{di} \odot \dot{\phi}_{ei} \odot \mathrm{S}_{\phi_{ei}}, \\ \dot{\alpha}_{wi}(t) &= \mathcal{H}^{-1} K_\phi \dot{\phi}_{ei} + \dot{w}_{di} + \dot{v}_{di} \odot y_{ei} + v_{di} \odot \dot{y}_{ei}. \end{aligned}$$

If the disturbances were known accurately, determining the control inputs would be trivial using

$$u_{vi}(t) = -K_z z_{vi}(t) + \dot{\alpha}_{vi}(t) - \delta_{vi}(t) \tag{10}$$
$$u_{wi}(t) = -K_z z_{wi}(t) + \dot{\alpha}_{wi}(t) - \delta_{wi}(t), \tag{11}$$

with $K_z > 0$. Unfortunately, in real-world applications, this is not the case. Hence, we leverage RBF-NNs approximator to estimate the unknown disturbances $\delta_{vi}(t)$ and $\delta_{wi}(t)$.

B. MAS Neuro-Adaptive Estimation

Theorem 1 allows us to estimate the disturbances $\delta_{vi}(t)$ and $\delta_{wi}(t)$, using a vector of *suitable activation functions* $\boldsymbol{\varphi}(z_i(t)) \in \mathbb{R}^\eta$ and an *ideal weight vector* $\boldsymbol{\omega}_i(t) \in \mathbb{R}^\eta$, such that, the best approximation of the unknown disturbances are written as,

$$\delta_{vi}(t) = \boldsymbol{\omega}_{vi}^T(t)\boldsymbol{\varphi}(z_{vi}(t)) + \varepsilon_{vi} \tag{12}$$
$$\delta_{wi}(t) = \boldsymbol{\omega}_{wi}^T(t)\boldsymbol{\varphi}(z_{wi}(t)) + \varepsilon_{wi}, \tag{13}$$

and corresponding estimates are expressed as

$$\hat{\delta}_{vi}(t) = \hat{\boldsymbol{\omega}}_{vi}^T(t)\boldsymbol{\varphi}(z_{vi}(t)) \tag{14}$$
$$\hat{\delta}_{wi}(t) = \hat{\boldsymbol{\omega}}_{wi}^T(t)\boldsymbol{\varphi}(z_{wi}(t)). \tag{15}$$

The approximation errors will be represented as $\tilde{\delta}_{vi}(t) = \delta_{vi}(t) - \hat{\delta}_{vi}(t)$ and $\tilde{\delta}_{wi}(t) = \delta_{wi}(t) - \hat{\delta}_{wi}(t)$. The weight estimation errors are $\tilde{\omega}_{vi}(t) = \omega_{vi}(t) - \hat{\omega}_{vi}(t)$ and $\tilde{\omega}_{wi}(t) = \omega_{wi}(t) - \hat{\omega}_{wi}(t)$, whose time-derivatives are written

$$\dot{\tilde{\omega}}_{vi}(t) = -\dot{\hat{\omega}}_{vi}(t) \text{ and } \dot{\tilde{\omega}}_{wi}(t) = -\dot{\hat{\omega}}_{wi}(t). \tag{16}$$

The associated adaptation laws $-\dot{\hat{\omega}}_{vi}(t)$ and $-\dot{\hat{\omega}}_{wi}(t)$ will be deduced from the stability analysis, which will be presented in a subsequent subsection. Based on this, the controllers for each agent (10) and (11) are rewritten with the estimation of the external disturbances as

$$u_{vi}(t) = -K_z z_{vi}(t) + \dot{\alpha}_{vi}(t) - \hat{\delta}_{vi}(t) \tag{17}$$
$$u_{wi}(t) = -K_z z_{wi}(t) + \dot{\alpha}_{wi}(t) - \hat{\delta}_{wi}(t). \tag{18}$$

C. Event-Based Control Design for a MAS

Event-triggered controllers are frequently employed in systems with limited processing capacity. The control inputs, $u_{vi}(t)$ and $u_{wi}(t)$ are updated asynchronously at time t_k. Subsequent sampling is triggered by specific events targeting the error behavior. Consequently, this approach leads to a reduction in computing resources and, by extension, a decrease in energy consumption. Accordingly, the neuro-adaptive control laws (17) and (18) are modified in such a way that $\forall t \in [t_k, t_{k+1})$

$$u_{vi}(t) = -K_z z_{vi}(t_k) + \dot{\alpha}_{vi}(t_k) - \hat{\delta}_1(t_k) \tag{19}$$

$$u_{wi}(t) = -K_z z_{wi}(t_k) + \dot{\alpha}_{wi}(t_k) - \hat{\delta}_2(t_k). \tag{20}$$

In this scheme, sampling errors arise due to the discretization process driven by the asynchronous triggered mechanisms which are expressed as:

$$\boldsymbol{\epsilon}_i(t) = \begin{bmatrix} \epsilon_{xi}(t) \\ \epsilon_{yi}(t) \\ \epsilon_{\phi i}(t) \\ \epsilon_{vi}(t) \\ \epsilon_{wi}(t) \end{bmatrix} = \begin{bmatrix} x_i(t) \\ y_i(t) \\ \phi_i(t) \\ v_i(t) \\ w_i(t) \end{bmatrix} - \begin{bmatrix} x_i(t_k) \\ y_i(t_k) \\ \phi_i(t_k) \\ v_i(t_k) \\ w_i(t_k) \end{bmatrix} \tag{21}$$

It is clear that the discretization error vanishes ($\boldsymbol{\epsilon}_i(t) = \mathbf{0}$) as $t = t_k$. Furthermore, those errors are upper-bounded as $||\boldsymbol{\epsilon}_i(t)|| \leq \bar{\boldsymbol{\epsilon}}_i$, that allow us to write the next errors,

$$\varrho_{vi}(t) = z_{vi}(t) - z_{vi}(t_k), \tag{22}$$

$$\varrho_{wi}(t) = z_{wi}(t) - z_{wi}(t_k). \tag{23}$$

These errors are also upper-bounded as $||\varrho_{vi}(t)|| \leq \bar{\varrho}_{vi}$ and $||\varrho_{wi}(t)|| \leq \bar{\varrho}_{wi}$. We create a sliding surface between our two error variables $\varrho_{si}(t) = \varrho_{vi}(t) + \lambda\varrho_{wi}(t)$. The upper bound of the discretization error of the sliding surface is

$$||\varrho_{si}(t)|| = ||\varrho_{vi}(t) + \lambda\varrho_{wi}(t)|| \leq ||\bar{\varrho}_{vi} + \lambda\bar{\varrho}_{wi}||. \tag{24}$$

The time instant t_k at which the control law is updated is governed by the trigger function. As long as the norm of the sliding surface cross a defined threshold $\iota > 0$, no event will occur and the control signal maintains its previous value. We define the trigger function as

$$\sigma_i = ||\varrho_{vi}(t) + \lambda\varrho_{wi}(t)|| - \iota \tag{25}$$

$$t_{k+1} = \inf\{t \in [t_k, \infty) : \sigma \geq 0\}, \tag{26}$$

just when $\sigma_i \geq 0$, the control outputs for the $i-th$ agent will be updated, the control-loop system is depicted in Fig.2.

D. Stability Analysis

Considering $\zeta_i = (x_{ei}, y_{ei}, \phi_{ei}, z_{vi}, z_{wi}, \tilde{\omega}_{vi}, \tilde{\omega}_{wi})$, we construct the Lyapunov function for the overall MAS,

$$V_i(\zeta_i) = \underbrace{\frac{1}{2}(x_{ei}^T x_{ei} + y_{ei}^T y_{ei} + \phi_{ei}^T \phi_{ei})}_{V_{1i}} + \underbrace{\frac{1}{2}(z_{vi}^T z_{vi} + z_{wi}^T z_{wi}) + \frac{1}{2\xi_v}\tilde{\boldsymbol{\omega}}_{vi}^T\tilde{\boldsymbol{\omega}}_{vi} + \frac{1}{2\xi_w}\tilde{\boldsymbol{\omega}}_{wi}^T\tilde{\boldsymbol{\omega}}_{wi}}_{V_{2i}}, \tag{27}$$

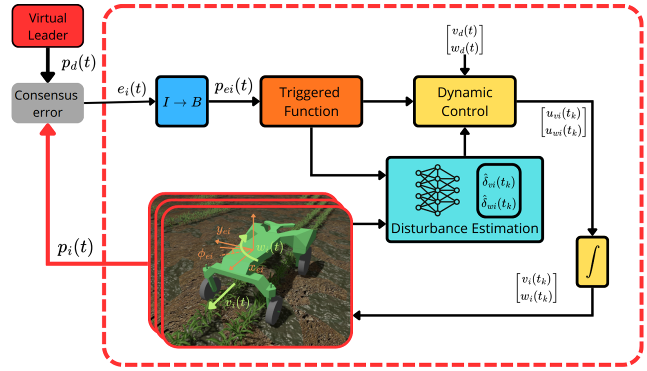

Fig. 2: Block diagram of the system.

where $\xi_v, \xi_w > 0$ are the learning/adaptive rates. Differentiating V_{1i} and using (6), (8) and (9):

$$\begin{aligned} \dot{V}_{1i} &= x_{ei}^T[w_i \odot y_{ei} + \mathcal{H}(-v_i + v_{di} \odot \mathrm{C}_{\phi_{ei}})] \\ &\quad + y_{ei}^T[-w_i \odot x_{ei} + \mathcal{H}(v_{di} \odot \mathrm{S}_{\phi_{ei}})] \\ &\quad + \phi_{ei}^T[\mathcal{H}(w_{di} - w_i)] \end{aligned} \tag{28}$$

$$\begin{aligned} \dot{V}_{1i} &\leq x_{ei}^T[\mathcal{H}(-v_i + v_{di} \odot \mathrm{C}_{\phi_{ei}})] \\ &\quad + \phi_{ei}^T[\mathcal{H}(w_{di} - w_i + y_{ei} \odot v_{di})] \end{aligned} \tag{29}$$

$$\dot{V}_{1i} \leq -x_{ei}^T K_x x_{ei} - \phi_{ei}^T K_\phi \phi_{ei}. \tag{30}$$

That give us $V_{1i} \leq 0$. Now Differentiating V_{2i},

$$\dot{V}_{2i} = z_{vi}^T \dot{z}_{vi} + z_{wi}^T \dot{z}_{wi} + \frac{1}{\xi_v}\tilde{\boldsymbol{\omega}}_{vi}^T\dot{\tilde{\boldsymbol{\omega}}}_{vi} + \frac{1}{\xi_w}\tilde{\boldsymbol{\omega}}_{wi}^T\dot{\tilde{\boldsymbol{\omega}}}_{wi}. \tag{31}$$

Using (6) and the approximations (14) and (15),

$$\begin{aligned} \dot{V}_{2i} &= z_{vi}^T(t)(u_{vi}(t) + \boldsymbol{\omega}_{vi}^T(t)\boldsymbol{\varphi}(z_{vi}(t)) + \varepsilon_{vi} - \dot{\alpha}_{vi}(t)) \\ &\quad + z_{wi}^T(t)(u_{wi}(t) + \boldsymbol{\omega}_{wi}^T(t)\boldsymbol{\varphi}(z_{wi}(t)) + \varepsilon_{wi} - \dot{\alpha}_{wi}(t)) \\ &\quad - \frac{1}{\xi_v}\tilde{\boldsymbol{\omega}}_{vi}^T(t)\dot{\hat{\boldsymbol{\omega}}}_{vi}(t) - \frac{1}{\xi_w}\tilde{\boldsymbol{\omega}}_{wi}^T(t)\dot{\hat{\boldsymbol{\omega}}}_{wi}(t) \end{aligned} \tag{32}$$

Introducing the control laws (19) and (20), and the time-derivatives of the weight estimation errors (16). Also considering that $\hat{\omega}_{vi}(t) \approx \hat{\omega}_{vi}(t_k)$ and $\hat{\omega}_{wi}(t) \approx \hat{\omega}_{wi}(t_k)$ as well as the approximation error, this leads us to

$$\begin{aligned} \dot{V}_{2i} &= -z_{vi}^T(t)K_z z_{vi}(t_k) + z_{vi}^T(t)\tilde{\boldsymbol{\omega}}_{vi}^T(t_k)\boldsymbol{\varphi}(z_{vi}(t_k)) \\ &\quad - z_{wi}^T(t)K_z z_{wi}(t_k) + z_{wi}^T(t)\tilde{\boldsymbol{\omega}}_{wi}^T(t_k)\boldsymbol{\varphi}(z_{wi}(t_k)) \\ &\quad + z_{vi}^T(t)\varepsilon_{vi} + z_{wi}^T(t)\varepsilon_{wi} \\ &\quad - \frac{1}{\xi_v}\tilde{\boldsymbol{\omega}}_{vi}^T(t_k)\dot{\hat{\boldsymbol{\omega}}}_{vi}(t_k) - \frac{1}{\xi_w}\tilde{\boldsymbol{\omega}}_{wi}^T(t_k)\dot{\hat{\boldsymbol{\omega}}}_{wi}(t_k) \end{aligned} \tag{33}$$

The following adaptive rules are used, $\dot{\hat{\boldsymbol{\omega}}}_{vi}(t_k) = \xi_{vi} z_{vi}^T(t)\boldsymbol{\varphi}(z_{vi}(t_k))$ and $\dot{\hat{\boldsymbol{\omega}}}_{wi}(t_k) = \xi_{wi} z_{wi}^T(t)\boldsymbol{\varphi}(z_{wi}(t_k))$, then,

$$\begin{aligned} \dot{V}_{2i} = &- z_{vi}^T(t)K_z z_{vi}(t_k) + z_{vi}^T(t)\varepsilon_{vi} \\ &- z_{wi}(t)^T K_z z_{wi}(t_k) + z_{wi}^T(t)\varepsilon_{wi}, \end{aligned} \tag{34}$$

Taking the errors (22), (23),

$$\begin{aligned} \dot{V}_{2i} = &- z_{vi}^T(t)K_z z_{vi}(t) + z_{vi}^T(t)(\varepsilon_{vi} + K_z\varrho_{vi}(t)) \\ &- z_{wi}^T(t)K_z z_{wi}(t) + z_{wi}^T(t)(\varepsilon_{wi} + K_z\varrho_{wi}(t)). \end{aligned} \tag{35}$$

By defining $\rho_{vi} = \varepsilon_{vi} + K_z \varrho_{vi}(t)$ and $\rho_{wi} = \varepsilon_{wi} + K_z \varrho_{wi}(t)$ and considering Young's inequality,

$$\begin{aligned}\dot{V}_{2i} \leq & - z_{vi}^T K_z z_{vi} + \frac{1}{2}||z_{vi}||^2 + \frac{1}{2}||\rho_{vi}||^2 \\ & - z_{wi}^T K_z z_{wi} + \frac{1}{2}||z_{wi}||^2 + \frac{1}{2}||\rho_{wi}||^2, \end{aligned} \tag{36}$$

as previously indicated the approximation errors are upper-bounded, as well as the discretization errors, hence, $||\rho_{vi}|| \leq \bar{\rho}_{vi}$ and $||\rho_{wi}|| \leq \bar{\rho}_{wi}$,

$$\begin{aligned}\dot{V}_{2i} \leq & - (\lambda_{min}(K_z) - 1/2) \left(||z_{vi}||^2 + ||z_{wi}||^2\right) \\ & + 1/2 \left(\bar{\rho}_{vi}^2 + \bar{\rho}_{wi}^2\right). \end{aligned} \tag{37}$$

Therefore,

$$\begin{aligned}\dot{V}_i(\zeta_i) \leq & - x_{ei}^T K_x x_{ei} - \phi_{ei}^T K_\phi \phi_{ei} + 1/2 \left(\bar{\rho}_{vi}^2 + \bar{\rho}_{wi}^2\right) \\ & - (\lambda_{min}(K_z) - 1/2) \left(||z_{vi}||^2 + ||z_{wi}||^2\right). \end{aligned} \tag{38}$$

Considering $\lambda_{min}(K_z) > 1/2$ the variables z_{vi} and z_{wi} are uniformly ultimately bounded. The trajectories converge and remain in the compact set: $\Omega = \left\{(z_{vi}, z_{wi}) : ||z_{vi}||^2 + ||z_{vi}||^2 \leq \frac{\bar{\rho}_{vi}^2 + \bar{\rho}_{wi}^2}{2\lambda_{min}(K_z) - 1}\right\}$.

E. Minimum Time Interval

In order to ascertain the minimum time interval required to evade the Zeno phenomenon, we take the time derivative of our sliding surface (24), also considering (22) and (23), and since t_k is constant $\forall t_k \in [t_k, t_{k+1})$, then,

$$\dot{\varrho}_{si}(t) = \dot{z}_{vi}(t) + \lambda \dot{z}_{wi}(t). \tag{39}$$

Taking into account our MAS model (6), and substituting our control inputs (19), (19), and the errors (22), (23), we obtain:

$$\begin{aligned}\dot{\varrho}_{si}(t) = & - K_z[z_{vi}(t) - \varrho_{vi}(t)] + \varepsilon_{vi} \\ & - \lambda K_z[z_{wi}(t) - \varrho_{wi}(t)] + \lambda \varepsilon_{wi} \end{aligned} \tag{40}$$

$$\begin{aligned}\dot{\varrho}_{si}(t) \leq & K_z||z_{vi}(t) + \lambda z_{vi}(t)|| \\ & + K_z||\varrho_{vi}(t) + \lambda \varrho_{wi}(t)|| + ||\varepsilon_{vi} + \lambda \varepsilon_{wi}|| \end{aligned} \tag{41}$$

$$\begin{aligned}\dot{\varrho}_{si}(t) \leq & K_z||\varrho_{si}(t)|| + K_z||z_{vi}(t) + \lambda z_{wi}(t)|| \\ & + ||\varepsilon_{vi} + \lambda \varepsilon_{wi}||. \end{aligned} \tag{42}$$

By defining $\Phi_i(t) = K_z||z_{vi}(t) + \lambda z_{wi}(t)|| + ||\varepsilon_{vi} + \lambda \varepsilon_{wi}||$, since the system is stable, the states $z_{vi}(t)$ and $z_{wi}(t)$ converge exponentially to zero, and the approximations errors ε_{wi} and ε_{wi} are bounded, we can take $\Phi_i(t) \leq K_z \bar{z}_i + \bar{\varepsilon}_i =: \Phi_i^{max}(t) < \infty$, therefore, $\dot{\varrho}_{si}(t) \leq K_z||\varrho_{si}(t)|| + \Phi_i^{max}(t)$ and the solution to the differential equation is:

$$\varrho_{si}(t) \leq \frac{\Phi_i^{max}(t)}{K_z}(\exp(K_z \tau) - 1). \tag{43}$$

According to event mechanism (25), an event is generated when $||\varrho_{si}(t)|| > \iota$, then,

$$\frac{\Phi_i^{max}(t)}{K_z}(\exp(K_z \tau) - 1) > \iota, \tag{44}$$

solving for τ, we can determine the minimum time interval to avoid Zeno behavior,

$$\tau_{min} = \frac{1}{K_z} \ln\left(1 + \frac{K_z \iota}{\Phi_i^{max}(t)}\right) > 0. \tag{45}$$

Since $K_z > 0$, $\iota > 0$ and $\Phi_i^{max}(t) > 0$, it follows that $\tau_{min} > 0$, Therefore, $t_{k+1} - t_k \geq \tau_{min} \forall k$, which rules out the Zero phenomenon.

V. Simulation and Results

A. MAS Configuration

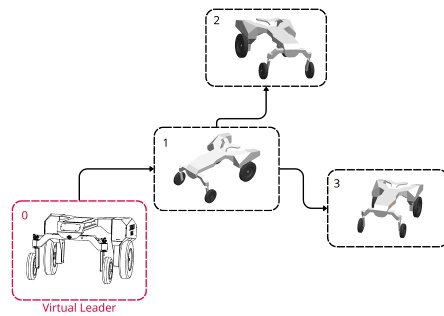

Fig. 3: MAS communication flow.

For this work we consider three Ackermann vehicles following a virtual leader which transmits the desired trajectory to the neighborhood by sharing the desired posture ($\boldsymbol{p}_d$) and the desired velocities (v_d and w_d). In Fig. 3, the utilized topology is illustrated, and the associated matrices pertaining to the communication flow between the vehicles are:

$$\mathcal{A} = \begin{bmatrix} 0 & 0 & 0 \\ 1 & 0 & 0 \\ 1 & 0 & 0 \end{bmatrix} \mathcal{B} = \begin{bmatrix} 1 & 0 & 0 \\ 0 & 0 & 0 \\ 0 & 0 & 0 \end{bmatrix}, \mathcal{D} = \begin{bmatrix} 0 & 0 & 0 \\ 0 & 1 & 0 \\ 0 & 0 & 1 \end{bmatrix},$$

$$\mathcal{L} = \begin{bmatrix} 0 & 0 & 0 \\ -1 & 1 & 0 \\ -1 & 0 & 1 \end{bmatrix}, \mathcal{H} = \begin{bmatrix} 1 & 0 & 0 \\ -1 & 1 & 0 \\ -1 & 0 & 1 \end{bmatrix}.$$

The agents maintain the following formation $\boldsymbol{p}_f = \begin{bmatrix} \mathbf{0}_n & \boldsymbol{y}_f & \mathbf{0}_n \end{bmatrix}^T$, with $\boldsymbol{y}_f = \begin{bmatrix} 0 & 5 & -5 \end{bmatrix}^T$. Finally, the initial conditions are set as follows $\boldsymbol{p}_{0_{A0}} = \begin{bmatrix} -25 & 12 & 0 \end{bmatrix}^T$, $\boldsymbol{p}_{0_{A1}} = \begin{bmatrix} -20 & 10 & 0 \end{bmatrix}^T$, $\boldsymbol{p}_{0_{A2}} = \begin{bmatrix} -22 & 15 & 0 \end{bmatrix}^T$ and $\boldsymbol{p}_{0_{A3}} = \begin{bmatrix} -18 & 5 & 0 \end{bmatrix}^T$.

B. Results and Discussion

The disturbances chosen for this test are

$$\delta_{vi} = [1.4\mathrm{H}(t-35),\ 1.2\cos(t),\ 0.6\sin(4t) + 0.9\cos(0.5t)]^T$$
$$\delta_{wi} = [0.4\sin(0.1t) + 0.3\cos(t),\ 0.9\cos(3t),\ 0.8\mathrm{H}(t-50)]^T,$$

where $\mathrm{H}(\star)$ is the Heaviside step function. Fig. 4 shows the desired trajectory of the virtual leader (formed using cubic splines) and the evolution of the posture $\boldsymbol{p}$ for each agent. In general, the agents start from the initial conditions to first achieve the desired formation $\boldsymbol{p}_f$ and then follow the virtual leader until the trajectory around the fields is completed. Fig. 5 shows the evolution of all state variables (x, y, ϕ, v and w), while Table I presents the mean absolute error μ for each state. Furthermore, Fig. 6 shows the tracking error associated with the perturbation estimation for each agent. Finally, Fig. 7 shows the evolution of the control signals, as well as the evolution of the events obtained for each agent.

	A_1	A_2	A_3
μ_x	0.0858	0.0749	0.0922
μ_y	0.0946	0.0298	0.0331
μ_ϕ	0.0405	0.0277	0.0234
μ_v	0.0172	0.0416	0.0451
μ_w	0.0233	0.0225	0.0337

TABLE I: Mean absolute error for each state variable

In the context of non-holonomic vehicles, angle normalization is necessary to ensure angles always remain within the range $(-\pi, \pi]$. This results in Fig. 5 displaying apparent fluctuations in the magnitude of the parameter ϕ, despite the fact that the true variation remains negligible. Consequently, this results in a significant increase in the desired angular velocity when the vehicle completes a 180 turn, as it is calculated as the time derivative of the desired angle. This abrupt change in the desired velocity is also reflected in the estimation produced by the neural network of each agent (Fig. 6) and, therefore, in the control output (Fig. 7), specifically at 58 and 91 seconds. The results show that 15.64%, 19.04% and 44.46% of all possible events were obtained, respectively, for agents A_1, A_2, and A_3. The occurrence of events is directly influenced by the disturbances faced by the agent. The frequency of events increases in response to faster disturbances, as evidenced by agent 3.

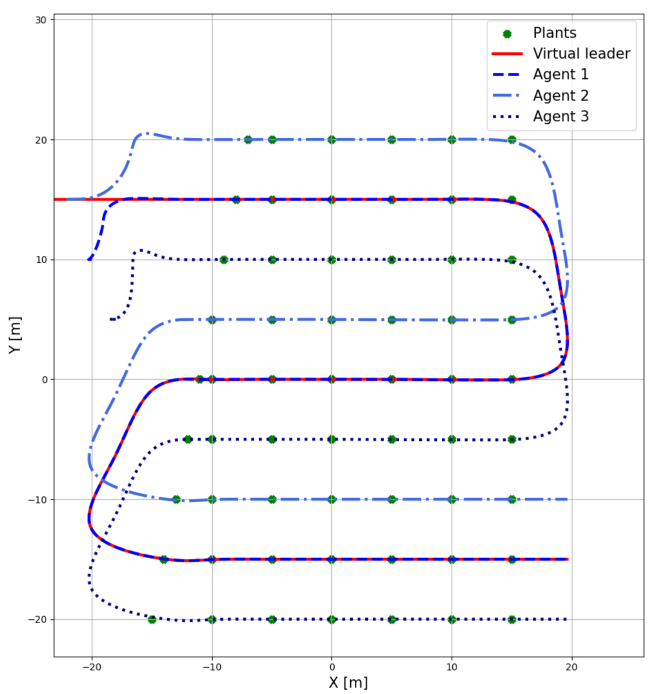

Fig. 4: Trajectory followed for the MAS.

VI. Conclusions

In this work, we addressed the tracking problem for a MAS composed of an ensemble of non-holonomic robots. By means of Backstepping methodology and neuro adaptive controller, we implemented a simplified dynamic controller to grapple exogenous disturbances arising from uneven terrain. Furthermore, using Lyapunov theory, we demonstrated the stability of the event-based control, as well as the avoidance of the Zeno phenomenon. The event-driven controller is used to reduce the computational cost

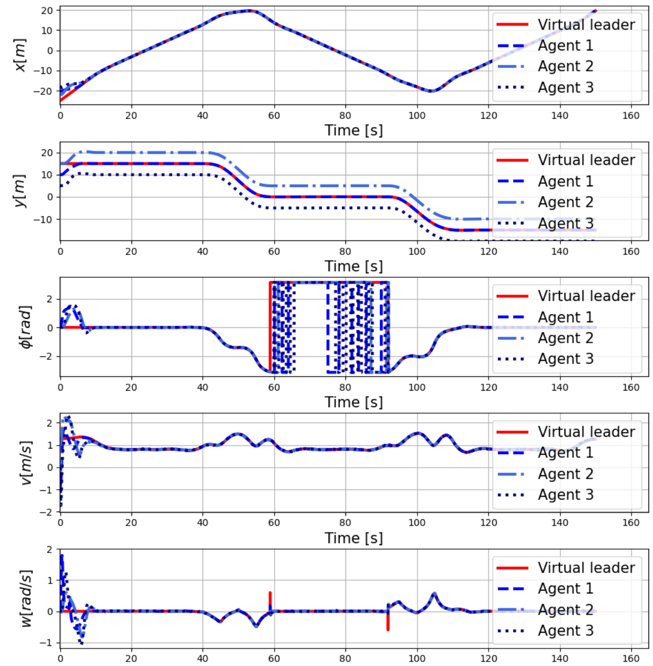

Fig. 5: Evolution of states (positions and velocities).

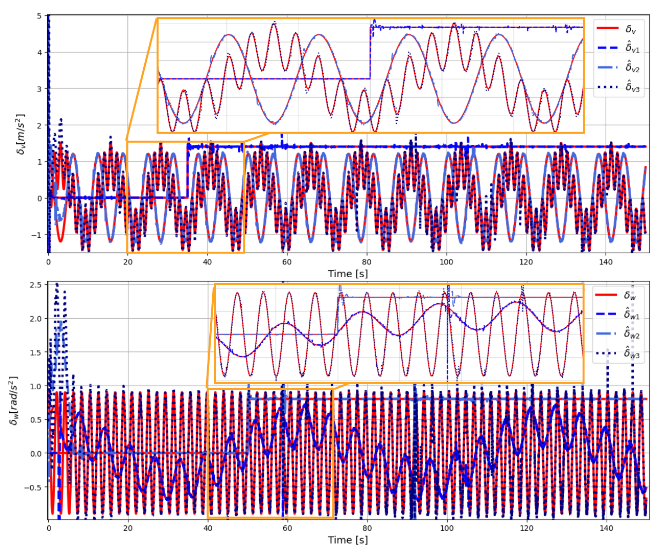

Fig. 6: Disturbance estimation.

required by the MAS, achieving a significant reduction in events throughout the simulation for each agent. The numerical results demonstrate and validate the effectiveness of the proposed control scheme. Further research stage includes conducting a 3D simulation in Gazebo and experimental results.

References

[1] Zhaohan Feng, Ruiqi Xue, Lei Yuan, Yang Yu, Ning Ding, Meiqin Liu, Bingzhao Gao, Jian Sun, Xinhu Zheng, and Gang Wang. Multi-agent embodied ai: Advances and future directions. *arXiv preprint arXiv:2505.05108*, 2025.

[2] Abdollah Amirkhani and Amir Hossein Barshooi. Consensus in multi-agent systems: a review. *Artificial Intelligence Review*, 55(5):3897–3935, 2022.

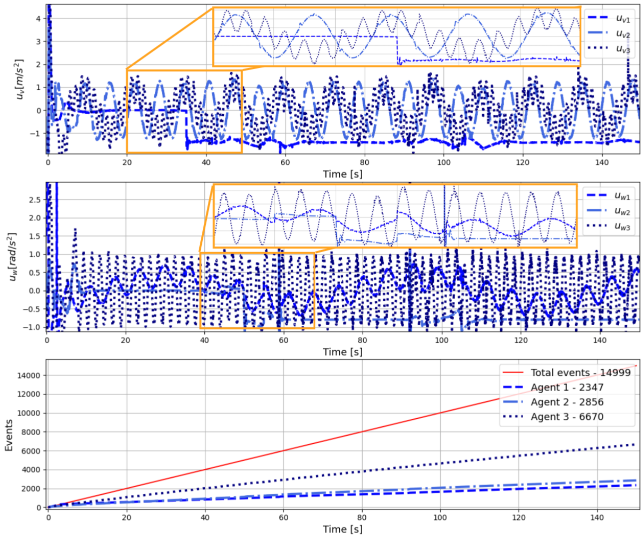

Fig. 7: Control signals for each agent and evolution of the events.

[3] Zhibin Zhu, Yanhui Yin, Fuyong Wang, Zhongxin Liu, and Zengqiang Chen. Practical robust fixed-time containment control for multi-agent systems under actuator faults. *Expert Systems with Applications*, 245:123152, 2024.

[4] Tianxing Chen, Xuebin Zhuang, Zhiwei Hou, and Hongbo Chen. Event-triggered adaptive sliding mode control for consensus of multiagent systems with unknown disturbances. *Scientific Reports*, 12(1):17473, 2022.

[5] Jose Guadalupe Romero and David Navarro-Alarcon. Robust integral consensus control of multi-agent networks perturbed by matched and unmatched disturbances: The case of directed graphs. *arXiv e-prints*, pages arXiv–2310, 2023.

[6] J. Escareno, J. U. Alvarez-Munoz, L. R. Garcia Carrillo, I. Rubio Scola, J. Franco-Robles, and O. Labbani-Igbida. Limbic system-inspired robust event-driven control for high-order uncertain nonlinear systems. *IEEE Control Systems Letters*, 8:3057–3062, 2024.

[7] Jihang Sui, Chao Liu, Ben Niu, Xudong Zhao, Ding Wang, and Bocheng Yan. Prescribed performance adaptive containment control for full-state constrained nonlinear multiagent systems: A disturbance observer-based design strategy. *IEEE Transactions on Automation Science and Engineering*, 22:179–190, 2025.

[8] Dajie Yao, Sergey Gorbachev, Chunxia Dou, Xiangpeng Xie, and Dong Yue. Adaptive tracking consensus control of nonlinear multiagent systems with predefined accuracy under disturbance observer. *IEEE Transactions on Systems, Man, and Cybernetics: Systems*, 53(7):4267–4278, 2023.

[9] Hongjing Liang, Guangliang Liu, Huaguang Zhang, and Tingwen Huang. Neural-network-based event-triggered adaptive control of non-affine nonlinear multiagent systems with dynamic uncertainties. *IEEE Transactions on Neural Networks and Learning Systems*, 32(5):2239–2250, 2020.

[10] Chengjie Huang, Zhi Liu, CL Philip Chen, and Yun Zhang. Adaptive fixed-time neural control for uncertain nonlinear multiagent systems. *IEEE Transactions on Neural Networks and Learning Systems*, 34(12):10346–10358, 2022.

[11] Jonatan Uziel Alvarez-Muñoz, Juan Antonio Escareno, Jeremy Chevalier, Steven Daix, and Ouiddad Labanni-Igbida. Wind-tolerant event-based adaptive sliding-mode control for vtol rotorcrafts multiagent systems. *IEEE Transactions on Aerospace and Electronic Systems*, 59(2):1400–1410, 2023.

[12] Xiang Li and Jing Zhu. Self-triggered control of multi-agent systems with external disturbances. *Frontiers in Control Engineering*, 3:835052, 2022.

[13] Long Jian, Yongfeng Lv, Rong Li, Liwei Kou, and Gengwu Zhang. Distributed disturbance observer-based containment control of multi-agent systems via an event-triggered approach. *Mathematics*, 11(10):2363, 2023.

[14] Jianchao He, Zijun Cheng, Tianshui Chang, Qidong Liu, and Yang Yang. Event-triggered finite-time tracking control for nonlinear systems via immersion and invariance techniques. *IEEE Transactions on Automation Science and Engineering*, 22:1606–1619, 2025.

[15] Xia Wu, Caisheng Wei, Zheng Wang, and Xin Ning. Distributed event-triggered fixed-time formation tracking control for multi-spacecraft systems based on adaptive immersion and invariance technique. *International Journal of Robust and Nonlinear Control*, 34(15):10105–10130, 2024.

[16] Béla Bollobás. *Modern graph theory*, volume 184. Springer Science & Business Media, 1998.

[17] Narsingh Deo. *Graph theory with applications to engineering and computer science*. Courier Dover Publications, 2016.

[18] Fan RK Chung. *Spectral graph theory*, volume 92. American Mathematical Soc., 1997.

[19] Jonathan L Gross and Jay Yellen. *Handbook of graph theory*. CRC press, 2003.

[20] Yutaka Kanayama, Yoshihiko Kimura, Fumio Miyazaki, and Tetsuo Noguchi. A stable tracking control method for an autonomous mobile robot. In *Proceedings., IEEE International Conference on Robotics and Automation*, pages 384–389. IEEE, 1990.

[21] ZHONG-PING JIANGdagger and Henk Nijmeijer. Tracking control of mobile robots: A case study in backstepping. *Automatica*, 33(7):1393–1399, 1997.